Case Studies in Thermal Engineering 8 (2016) 260–276

Contents lists available at ScienceDirect

Case Studies in Thermal Engineering

journal homepage: www.elsevier.com/locate/csite

Performance evaluation of gauze packing for liquid desiccant dehumidification system

A.S.A. Mohamed [a], M.S. Ahmed [a,*], A.A.M. Hassan [b], M. Salah Hassan [b]

[a] Department of Mechanical Engineering, Faculty of Industrial Education, Sohag University, Egypt
[b] Department of Mechanical Power Engineering and Energy, Faculty of Engineering, Minia University, Egypt

ARTICLE INFO

Article history:
Received 15 April 2016
Received in revised form
15 July 2016
Accepted 23 August 2016
Available online 29 August 2016

Keywords:
Liquid desiccant
Cross flow
Humidity reduction
Humidity effectiveness
Pressure drop

ABSTRACT

Desiccant systems have found applications in a very large variety of industrial and daily usage products including the new HVAC installations. The dehumidifier is one of the essential parts of those systems, which severely affects the whole system performance. This paper theoretically and experimentally studies the performance of the cross flow dehumidifier, which has been less studied than the counter flow dehumidifier, although it is more applicable in practice. Channel gauze structured packing was used in the dehumidifier and a LiCl aqueous solution was used as the liquid desiccant. The humidity reduction and dehumidifier effectiveness were adopted as the dehumidifier performance indices. The effects of the dehumidifier inlet parameters, including inlet air and desiccant flow rates, inlet air and desiccant temperature, inlet desiccant concentration and inlet air humidity ratio, on the two indices were investigated. The characteristics of the dehumidifier performance agreed well with the other studies reported in the open literature.

1. Introduction

Dehumidification is the process of removal of water vapor from moist air. It can be achieved by either cooling or increasing the pressure of air or by absorption/adsorption of moisture by a solid or liquid material (called a desiccant). The two methods, cooling and increasing the pressure of air, require high energy consumption.

Recently, a number of hybrid air conditioning systems have been proposed, in which liquid and solid desiccants are used to meet the latent heat load. A liquid desiccant system is preferable because of its operational flexibility, ability to absorb inorganic and organic contaminants from air [1–4] and its ability also to operate under a relatively low regeneration temperature. Besides, using of brine as absorbents is frequently environmentally friend as it does not cause ozone depletion [5].

The liquid desiccant air-conditioning system has been proposed as an alternative to the conventional vapor compression cooling systems to control air humidity, especially in hot and humid areas, due to its advantage in removing the latent load as well as the potential to remove a number of pollutants from the air stream [6–8]. The removal of moisture from the air depends on the difference in water vapor pressure held by the desiccant and that of water vapor present in the air [9].

The main components of a liquid desiccant system are two gas–liquid contactors, a dehumidifier, and a regenerator. The air is dehumidified by being in contact with concentrated solution in a dehumidifier. The solution is diluted during the dehumidification process, and needs to be regenerated before being reused. There are two types of gas–liquid contactors, namely, structured packing and random packing [10–12].

* Corresponding author.
E-mail address:

http://dx.doi.org/10.1016/j.csite.2016.08.005
2214-157X/

Nomenclature

a	specific area of packing per volume (m^2/m^3)
$C_{p,\ a}$	specific heat of liquid desiccant (kJ/kg K)
D_{eq}	equivalent diameter (m)
H	height of the cross flow dehumidifier (m)
k	thermal conductivity (kW/mK)
L	length of cross flow dehumidifier (m)
Le	Lewis number, $(\alpha/\alpha_m C_{p,a})$
$\dot{m}_a$	air flow rate (kg/s)
$\dot{m}_s$	liquid desiccant flow rate (kg/s)
Nu	Nusselt number, $\alpha D_{eq}/K$
P	total pressure (kPa)
Pr	Prandtl number, $\mu C_{p,a}/K$
P_v	vapor pressure (kPa)
Re	Reynolds number, $\rho u D_{eq}/\mu$
R_v	characteristic gas constant for water vapor (kJ/kg K)
T	temperature (°C)
u	air velocity (m/s)
W	width of cross flow dehumidifier (m)
X	concentration (mass ratio of desiccant to solution) of the liquid desiccant (%)

Greek symbols

α	heat transfer coefficient (kW/m^2 °C)
α_m	mass transfer coefficient (kg/m^2 s)
ε_m	dehumidifier effectiveness (%)
ζ	pressure drop coefficient per meter in flow direction (1/m)
ρ	density (Kg/m^3)
ω_a	humidity ratio of air ($g_{w.v}/kg_{d.a}$)
ω_e	humidity ratio of air in equilibrium with liquid desiccant ($g_{w.v}/kg_{d.a}$)

Subscripts

a	air
d.b	dry bulb
e	equilibrium
g	gas
i	inlet
m	mixture
o	outlet
s	liquid desiccant solution
v	vapor
w	water
w.b	wet bulb

The use of liquid desiccants offers an important advantage; in addition to reducing humidity, the quality of the air can be controlled through the co-absorption of pollutants into the solution. However, direct-contact liquid desiccant air-conditioning systems have the risk of carry-over of aerosol droplets to the supply airstream, which may cause health problems for occupants and corrosion of the ducting system. The desiccant carry-over problem can be eliminated by using a liquid-to-air membrane energy exchanger (LAMEE). The LAMEE is a novel energy exchanger, in which air and desiccant solution streams are separated using semi-permeable membranes [13–18]. These membranes allow simultaneous heat and moisture transfer between the air and desiccant solution streams, but do not allow the transfer of any liquid droplets, and thus eliminate the desiccant carry-over problem. A new liquid-to-air (LAMEE) was developed and progress has been made on the research and applications of LAMEEs in building HVAC systems [13–16].

The dehumidifier and regenerator can be divided into adiabatic and internally cooled types. In the adiabatic module, only air and desiccant exchange heat and mass (moisture content). The adiabatic dehumidifiers can afford large air-desiccant contacting area with relatively simple geometry configuration. Internally cooled or heated liquid desiccant–air contact units can be used for effective air dehumidification or desiccant regeneration, respectively [19–23]. Since the desiccant is cooled/heated synchronously, as it contacts humid/dry air, and thus maintains its low/high surface vapor pressure. Abdel Salam [19] presented an experimental data for a new 3-fluid liquid to air membrane energy exchanger which uses cooling/heating water to cool/heat the desiccant solution.

Packing materials is the place where mass transfer occurs between falling film of the LD and inlet air. Hence, The packing material is one of the most important factors affecting the performance of the dehumidification process . The structured packing, namely gauze-type has been selected for a lot of advantages such as low pressure drop, sensitivity to fouling, liquid holdup, ease of handling high or low desiccant flow rate, resistance to corrosion, and reasonable cost. Many studies provided rigorous models for predicting the pressure drop in both structured and random packing materials, and most of them revealed that the structured packing has the lower pressure drop and higher capacity compared with random packing. This study, therefore, investigates the performance of a cross-flow liquid desiccant dehumidification system. Structured gauze packing slides have been selected; the installation and pressure drop are more convenient, compared with other packing.

2. Experimental facility

2.1. Description of the liquid desiccant dehumidifier

The schematic and photograph of the structure packing and the components of the experimental cross-flow packed bed dehumidifier are shown in Fig. 1a and b respectively. The main apparatus consists of gauze packing slides (1), dilute solution

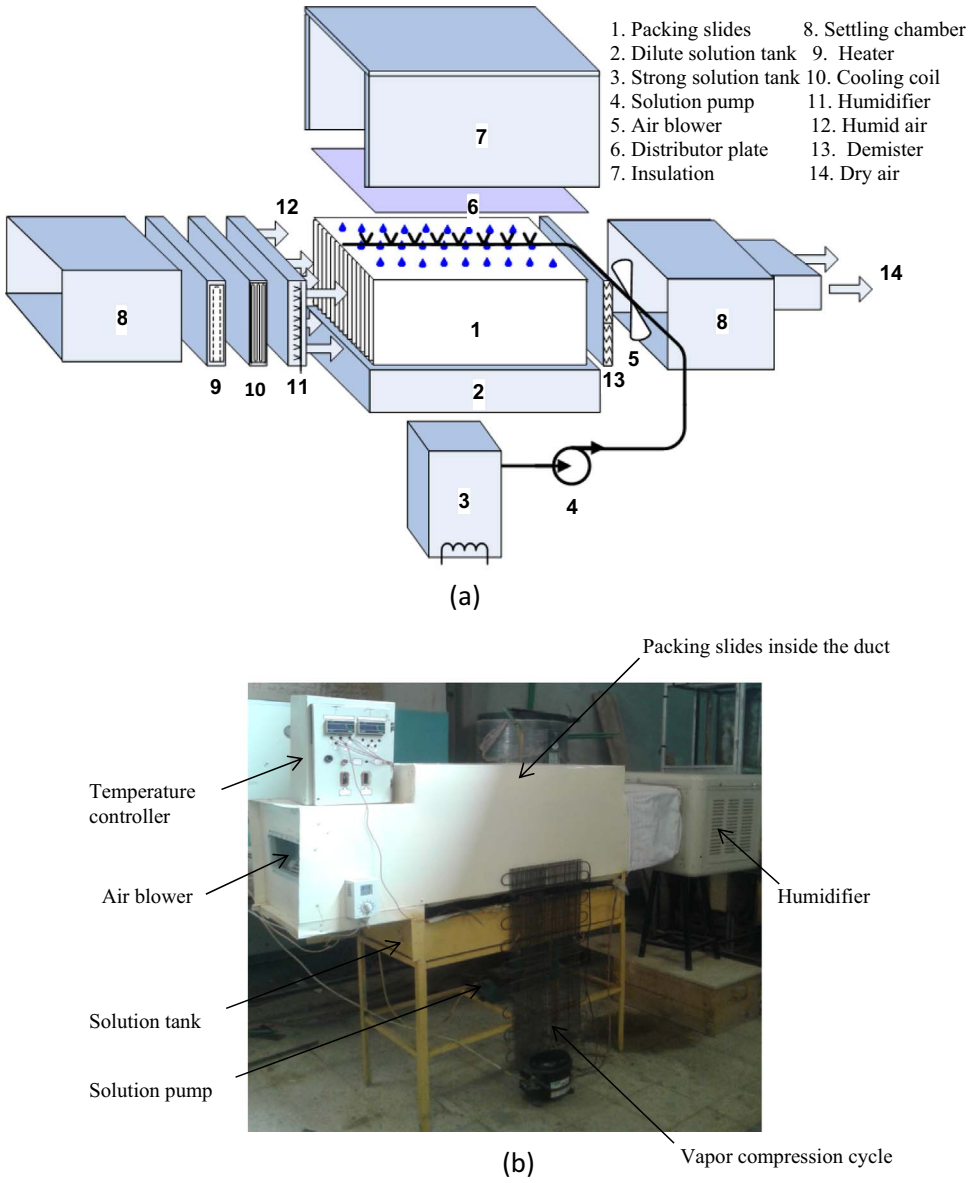

Fig. 1. Dehumidification system: (a) schematic of experimental set-up and (b) photo of experimental set-up.

tank (2), strong solution tank (3), solution pump (4), air blower (5), distributor plate (6), settling chamber (8), electric heater (9), cooling coil (10), and humidifier (11).

Photo of structural gauze packing slides, shown in Fig. 2, is placed inside the dehumidifier to enlarge the heat and mass transfer area between the air and liquid desiccant. Fresh, unused lithium chloride was stored in a tank (3), and its temperature was adjusted by circulating cold or warm water through a submerged stainless steel coil. The liquid desiccant solution is withdrawn by pump (4) from this tank and sprayed from the top by a sprinkler to affect a falling film at the surface of the slides structural packing wall and air is introduced into the dehumidifier from the left. The electric heater (9), cooling coil (10) and humidifier (11) have been fixed at the place of air entrance for adjusting the conditions of inlet air.

The configuration of gauze packing slides is shown in Fig. 1a. It is porous and durable for repeated wetting and drying and has very large pore surface for a given packing volume. To begin, the process air is fan driven (5) through the channel where the moisture of the air is absorbed, and both the air and the liquid desiccant become warm due to the effect of the mixing heat in the air dehumidification. The liquid desiccant solution becomes dilute at the same time and has to be regenerated to maintain a dehumidification cycle.

Fig. 2. Photo of gauze packing slides.

2.2. Measuring instruments

Operating parameters of desiccant and air were measured before and after the dehumidifier to investigate the performance of dehumidifier. The measured desiccant parameters included flow rate, temperature and concentration. The tested air parameters included flow rate, dry bulb temperature and humidity ratio. An orifice meter was used to measure the desiccant flow rate. Then desiccant concentration could be found by the measured desiccant density and temperature based on the physical property of the LiCl desiccant [24]. The temperatures were measured using PT100, and the temperature readings were scanned and recorded by the data acquisition system (Agilent13970 A). A digital hot-wire anemometer was used to measure velocity. The air humidity ratio was derived from the measured dry-bulb and wet-bulb temperatures, and the pressure drop was measured by inclined differential manometer. The measurement devices and corresponding accuracies are shown in Table 1.

3. Experimental conditions

Photo of gauze type structured packing is shown in Fig. 2, in which the cross flowing air and desiccant exchanged heat and moisture. The system used slides channel structured packing with the specific surface area of 400 m^2/m^3. Its height, length and width were 0.4 m, 1.0 m and 0.4 m, respectively. These slides are positioned vertically to form the air channels, which will enhance the mass transfer process and reduce the pressure drop. The distance between the slides of gauze is 5 mm.

Different types of liquid desiccants are available in the market such as LiBr, $CaCl_2$, etc. In most applications the general properties requirements are low vapor pressure, the capability of maintaining dehydrating ability over a considerable range of concentration, non-corrosive, low viscosity, high density, low crystallization point, low regeneration temperature, low cost and safe. All requirements are not answered by any desiccant, but investigations found that LiCl is the most suitable one

Table 1
Specification of the different measuring devices.

Parameters	Devices	Accuracy	Operational range
Air flow velocity	Hot-wire anemometer	± 0.1 m/s	0–10 m/s
Air dry bulb temperature	PT100	± 0.2 °C	0–100 °C
Air wet bulb temperature	PT100	± 0.2 °C	0–100 °C
Desiccant flow rate	Orifice meter	± 2.5%	Cd = 0.63
Desiccant temperatures	PT100	± 0.2 °C	0–100 °C
Desiccant density	Specific gravity hydrometer	± 1 kg/m^3	1000–1700 kg/m^3

Table 2
Inlet values of dehumidification condition.

Inlet parameters	Unit	Steady state inlet values
Air temperature	°C	33
Air moisture	g/kg	18
Air flow rate	kg/s	0.1
Desiccant temperature	°C	25
Desiccant flow rate	kg/s	0.2
Desiccant concentration	%	38

as it has a lot of these properties. So, LiCl solution with lower surface vapor pressure was chosen to be used in the experiment. Experiments have been conducted with the following parameters, shown in Table 2.

The system was run by the inlet value of parameters in Table 2 until it reached steady state, and then data measurement were carried out while only one parameter was changed. When it is finished, the value of the parameter was restored to initial value, and then similar operations were made with other parameters.

4. Theoretical model

The schematic of the cross-flow packed bed dehumidifier is shown in Fig. 3a, with the height, length and width of H, L and W, respectively. Since the conditions of desiccant and air are uniform along the y direction in Fig. 3a, only their values changes on the x–z plane are studied, as shown in Fig. 3b.

The steady state porous medium volume averaged conservation equations of mass, momentum, and air fraction, with flow, heat, and mass transfer resistances, are written in the one dimensional system. This results in the following set of equations:

1. Conservation of air mass fraction

$$\frac{d\rho_g u}{dx}=0$$
$$\rho_g\frac{du}{dx}+u\frac{d\rho_g}{dx}=0\rho_g\frac{du}{dx}=-u\frac{d\rho_g}{dx} \tag{1}$$

2. Mass conservation equation for the vapor

$$\frac{d\rho_v u}{dx}=-\alpha_m a(\omega_a-\omega_e)=-\frac{\alpha_m}{\rho_g}\alpha\left(\rho_v-\rho_{v,e}\right)=C_1$$

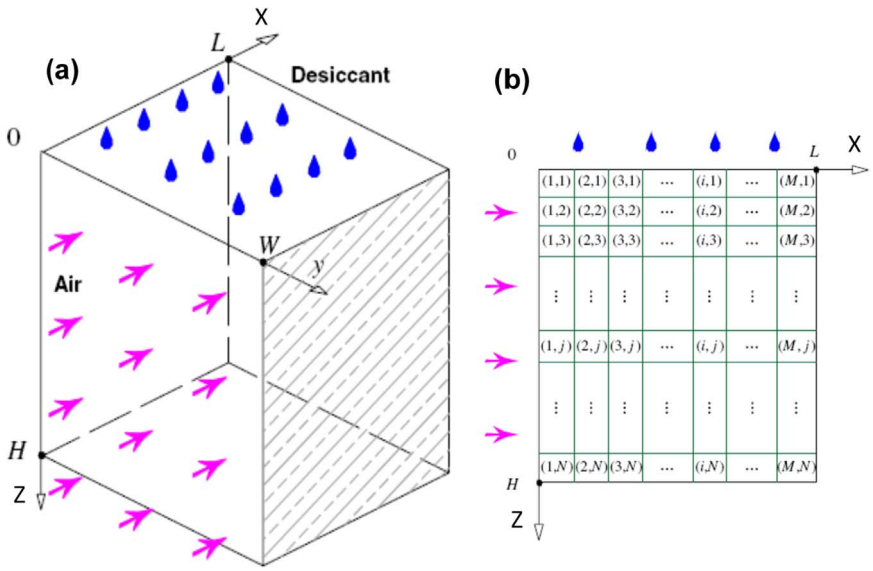

Fig. 3. Schematic of cross-flow packed bed dehumidifier: (a) three dimensional view and (b) sectional view.

$$\rho_v \frac{du}{dx} + u\frac{d\rho_v}{dx} = C_1\rho_v \frac{du}{dx} = -u\frac{d\rho_v}{dx} + C_1 \tag{2}$$

where:

α_m= mass transfer coefficient, kg/m^2 s
ω_a=air humidity ratio, $g_{w.v}/kg_{d.a}$
ω_e=humidity ratio of air in equilibrium with liquid desiccant, $g_{w.v}/kg_{d.a}$

3. Momentum conservation equation for the air

$$\frac{d\rho_a u^2}{dx} = \frac{d}{dx}\left(\rho_v u + \rho_g u\right)u = u\frac{d\left(\rho_v u + \rho_g u\right)}{dx} + \left(\rho_v u + \rho_g u\right)\frac{du}{dx}$$

$$= u\frac{\rho_v u}{dx} + u\frac{d\rho_g u}{dx} + \left(\rho_v + \rho_g\right)u\frac{du}{dx}$$

$$= C_1 u + \left(\rho_v + \rho_g\right)u\frac{du}{dx} = -\frac{dp}{dx} - \zeta\frac{\rho_a u^2}{2} + C_1 u$$

$$\frac{d\rho_a u^2}{dx} = -\frac{dp}{dx} - \zeta\frac{\rho_a u^2}{2} + C_1 u$$

where
ζ pressure drop coefficient per meter in flow direction, 1/m

$$\left(\rho_v + \rho_g\right)u\frac{du}{dx} = -\frac{dp}{dx} - \zeta\frac{\rho_a u^2}{2} \tag{3}$$

4. Equation of state

The air and vapor is assumed to behave as a perfect gas.

$$P = \rho_g R_g T_a + \rho_v R_v T_a = T_a\left(\rho_g R_g + \rho_v R_v\right)$$

$$\therefore \frac{dp}{dx} = \left(R_g\rho_g + R_v\rho_v\right)\frac{dT_a}{dx} + T_a\left(R_g\frac{d\rho_g}{dx} + R_v\frac{d\rho_v}{dx}\right)$$

$$= C_2 + C_3\frac{d\rho_g}{dx} + C_4\frac{d\rho_v}{dx}$$

where:

$$C_2 = \left(R_g\rho_g + R_v\rho_v\right)\frac{dT_a}{dx}$$

$$C_3 = R_g T_a$$

$$C_4 = R_v T_a$$

$$\left(\rho_v + \rho_g\right)u\frac{du}{dx} = -C_2 - C_3\frac{d\rho_g}{dx} - C_4\frac{d\rho_v}{dx} - \zeta\frac{\rho_a u^2}{2}$$

from Eq. (1)

$$\frac{du}{dx} = -\frac{u}{\rho_g}\frac{d\rho_g}{dx}$$

from Eq. (2)

$$\frac{du}{dx}=-\frac{u}{\rho_g}\frac{d\rho_v}{dx}+\frac{C_1}{\rho_v}-u^2\frac{d\rho_v}{dx}+C_1u-u^2\frac{d\rho_g}{dx}=-C_2-C_3\frac{d\rho_g}{dx}-C_4\frac{d\rho_v}{dx}+ \tag{4}$$

where:-

$$C_5=-\zeta\frac{\rho_a u^2}{2}$$

$$\because -\frac{u}{\rho_g}\frac{d\rho_g}{dx}=-\frac{u}{\rho_v}\frac{d\rho_v}{dx}+\frac{C_1}{\rho_v}$$

$$\therefore \frac{d\rho_g}{dx}=\frac{\rho_g}{\rho_v}\frac{d\rho_v}{dx}-\frac{\rho_g}{\rho_v}\frac{C_1}{u}\therefore \frac{d\rho_g}{dx}=C_6\frac{d\rho_v}{dx}+C_7 \tag{5}$$

where:-

$$C_6=\frac{\rho_g}{\rho_v}$$

$$C_7=\frac{\rho_g}{\rho_v}\frac{C_1}{u}$$

from Eq. (4)

$$-u^2\frac{d\rho_v}{dx}+C_1u-u^2\frac{d\rho_g}{dx}+C_2+C_3\frac{d\rho_g}{dx}+C_4\frac{d\rho_v}{dx}-C_5=0$$

$$\therefore \left(-u^2+C_4\right)\frac{d\rho_v}{dx}=-\left(-u^2+C_3\right)\frac{d\rho_g}{dx}-C_1u-C_2+C_5$$

$$\therefore \frac{d\rho_v}{dx}=\frac{-\left(-u^2+C_3\right)d\rho_g}{\left(-u^2+C_4\right)}+\frac{\left(-C_1u-C_2+C_5\right)}{\left(-u^2+C_4\right)}\frac{d\rho_v}{dx}=C_8\frac{d\rho_g}{dx}+C_9 \tag{6}$$

where:-

$$C_8=\frac{-\left(-u^2+C_3\right)}{\left(-u^2+C_4\right)}$$

$$C_9=\frac{-\left(-C_1u+C_2+C_5\right)}{\left(-u^2+C_4\right)}$$

$$\frac{d\rho_v}{dx}=C_8\left(C_6\frac{d\rho_v}{dx}+C_7\right)+C_9=C_8C_6\frac{d\rho_v}{dx}+C_8C_7+C_9=C_{10}\frac{d\rho_v}{dx}+C_{11}$$

$$\left(1-C_{10}\right)\frac{d\rho_v}{dx}=C_{11}\therefore \frac{d\rho_v}{dx}=\frac{C_{11}}{1-C_{10}}=C_{12} \tag{7}$$

where:

$$C_{10}=C_6C_8$$

$$C_{11}=C_7C_8+C_9$$

$$C_{12}=\frac{C_{11}}{1-C_{10}}$$

from Eqs. (6) and (7)

$$C_{12}=C_8\frac{d\rho_g}{dx}+C_9$$

$$\therefore \frac{d\rho_g}{dx}=\frac{C_{12}-C_9}{C_8}=C_{13} \tag{8}$$

Eqs. (1) and (8) are combined to obtain:

$$\frac{du}{dx} = \frac{-u}{\rho_g} C_{13} \tag{9}$$

An energy balance on the air and liquid desiccant gives:

$$\frac{dT_a}{dx} = \frac{-\alpha a(T_a - T_s)}{\dot{m}_s C_{p,s} H} = \frac{-\alpha a(T_a - T_s)}{\rho_a u C_{p,a}} \tag{10}$$

$$\frac{dT_s}{dz} = \frac{A}{\dot{m}_s C_{p,s} H}\left[\left(\lambda - C_{p,s} T_s\right)\alpha_m(\omega_a - \omega_e) + \alpha(T_a - T_s)\right] \tag{11}$$

The heat and mass transfer coefficient between the air and the desiccant solution was given as follows [25]:
For laminar flow:

$$Nu = 1.86(RePr)^{1/3}\left(\frac{D_{eq}}{L}\right)^{1/3} \tag{12}$$

$$D_{eq} = \frac{4W_c H_c}{2(W_c + H_c)} = \frac{2W_c H_c}{W_c + H_c} \tag{13}$$

$$\alpha = \frac{Nuk_a}{D_{eq}} \tag{14}$$

$$Le = \frac{\alpha}{\alpha_m C_{p,a}} \tag{15}$$

Boundary conditions are required to obtain the solutions of the above equations.

$$\rho_g = \rho_{g,i},\ \rho_v = \rho_{v,i},\ u = u_i,\ T_a = T_{a,i} \text{ at } X=0 T_s = T_{s,i},\ m_s = m_{s,i} \text{ at } Z=0 \tag{16}$$

Eqs. (7)–(11) were solved numerically by fourth order Runge Kutta method using Fortran program. With known inlet air and desiccant parameters, solving the equations gives the air outlet parameters.

Vapor pressure is an important property which determines the air humidity ratio in equilibrium with the desiccant at the interface. In this study, a second order polynomial was used and the coefficients were obtained from a curve fit using data from [26]:

$$P_v = \left(a_o + a_1 T_s + a_2 T_s^2\right) + \left(b_o + b_1 T_s + b_2 T_s^2\right)X + \left(c_o + c_1 T_s + c_2 T_s^2\right)X^2 \tag{17}$$

where the constants are given for the dehumidification process as:

a_o	**a_1**	**a_2**
4.58208	−0.159174	0.0072594
b_o	**b_1**	**b_2**
−18.3816	0.5661	−0.019314
c_o	**c_1**	**c_2**
21.312	−0.666	0.01332

5. Heat and mass transfer performance and efficiency analysis

The mass transfer performance of the dehumidifier was evaluated in terms of the humidity reduction [27–29] and the dehumidifier effectiveness [29]. The humidity reduction, $\Delta\omega_a$, was calculated by Eq. (18). The dehumidifier effectiveness, ε_m, is the ratio of the measured humidity ratio difference of the air passing through the dehumidifier to its ideal conditions variation, as given by Eq. (19). Validation of the experimental work with modeling is conducted upon the parameters affecting the dehumidification processes.

$$\Delta\omega_a = \omega_{a,i} - \omega_{a,o} \tag{18}$$

$$\varepsilon_m = \frac{\omega_{a,i} - \omega_{a,o}}{\omega_{a,i} - \omega_{e,i}} \tag{19}$$

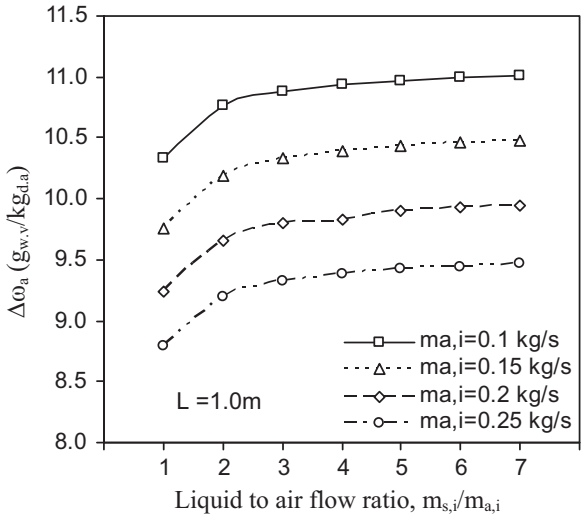

Fig. 4. Influence of inlet liquid to air flow ratio on humidity reduction.

5.1. Experimental results

5.1.1. Optimum liquid desiccant to air flow rate ratio

To decrease the pumping cost of Liquid desiccant and air through the dehumidifier, the optimum liquid desiccant to air flow ratio with respect to moisture removal must be determined.

Fig. 4, shows the measured humidity reduction through the dehumidifier, $\Delta\omega_a$, during the tests against the liquid desiccant to air flow ratio. Fig. 4 shows that the humidity reduction increases significantly with the liquid to air flow rate ratio until it reaches 2.0. When the ratio exceeds 2.0, the gain in humidity reduction is negligible. The figure also shows that, at any value of liquid to air mass flow rate ratio, the humidity reduction decreases linearly with increasing the air flow rate. This figure shows that for packed section with 1 m long, the optimum flow ratio is 2.0.

5.2. Validation of the experimental work with modeling

Six inlet parameters of the air and desiccant, including desiccant and air flow rates, desiccant and air temperature, desiccant concentration and air humidity ratio, surely influence the dehumidifier performance. The effect of each parameter is analyzed as follows.

5.2.1. Effect of inlet desiccant flow rate on the performance

The increase of the liquid flow rate resulted in an increase in humidity ratio reduction and humidity effectiveness, as shown in Fig. 5a and b with L=1.0 m and L=0.5 m, respectively. The effect can be explained as follows. With the desiccant flow rate increasing, the variation of the desiccant concentration and temperature through the dehumidifier decreased. As a result, increasing the desiccant flow rate decreased the variation of the surface vapor pressure of the desiccant through the dehumidifier and, hence, increased the average water vapor pressure difference between the desiccant and air in the dehumidifier. Based on the above three aspects, increasing the desiccant flow rate increased the humidity reduction and the dehumidifier effectiveness. From Fig. 5a and b, it is notable that increasing the length of the packing slides from L=0.5 m to L=1.0 m enhanced the humidity reduction and dehumidifier effectiveness about 1.29 times. Fig. 5b shows that the difference in humidity effectiveness between the current work and Gao and Liu [12] at lower desiccant flow rate may return to the reason that the packing material used in the current work has a wettability better than Gao and Liu.

5.2.2. Effect of inlet desiccant concentration on the performance

Fig. 6a with L=1.0 m and Fig. 6b with L=0.5 m show the effect of inlet desiccant concentration on the dehumidifier performance. As shown in the figures, the humidity reduction increased remarkably with increasing inlet desiccant concentration, whereas a slight increase was observed in the humidity effectiveness with it. The reason may be as follows. Increasing the inlet desiccant concentration decreased the desiccant surface vapor pressure and, so, increased the average water vapor pressure difference between the desiccant and air in the dehumidifier, leading to lower air outlet humidity ratio and, hence, higher humidity reduction. Both $\omega_{e,i}$ and $\omega_{a,o}$ in Eq. (19) decreased with increasing inlet desiccant concentration. They offset each other, resulting in slight effect on the dehumidifier effectiveness. From Fig. 6a and b, it is clear that increasing the length of gauze packing slides from L=0.5 m to L=1.0 m increased the humidity reduction and dehumidifier effectiveness about 28%. Fig. 6b shows also that a good agreement was observed with Gao and Liu [12] relating to the dehumidifier effectiveness at L=0.5 m.

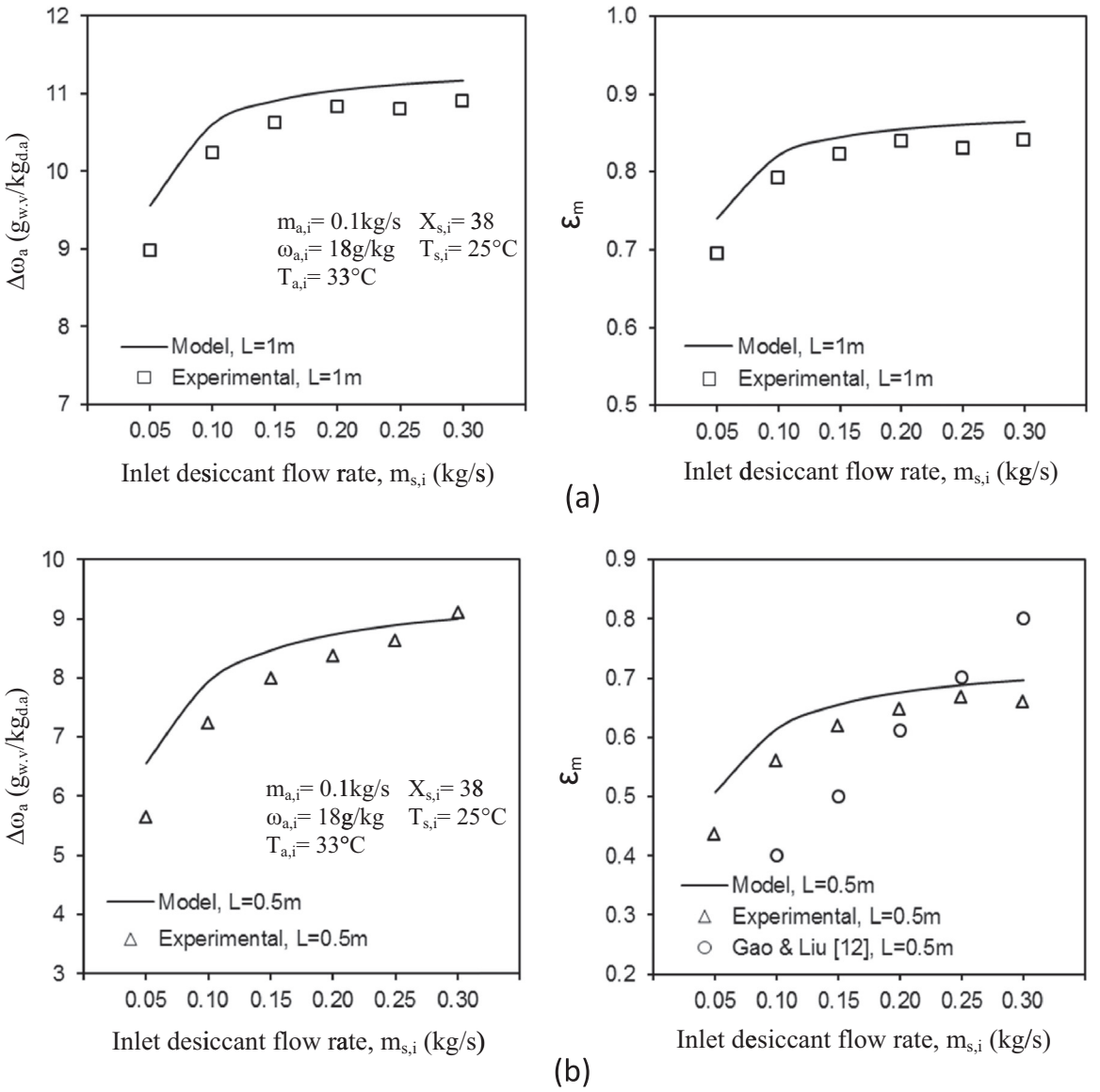

Fig. 5. Influence of inlet desiccant flow rate on humidity reduction and dehumidifier effectiveness: (a) L=1.0 m and (b) L=0.5 m.

5.2.3. Effect of inlet desiccant temperature on the performance

The effect of inlet desiccant temperature on the humidity reduction and dehumidifier effectiveness is shown in Fig. 7a and b. As indicated by the figures, the humidity reduction decreased significantly, whereas the humidity effectiveness is affected slightly with increasing inlet desiccant temperature. This may be explained as follows. Increasing the desiccant temperature increased the surface vapor pressure of the desiccant and, so, decreased the average water vapor pressure difference between the air and desiccant in the dehumidifier, which led to higher air outlet humidity ratio and, hence, lower moisture removal rate. As for humidity effectiveness, increasing the inlet desiccant temperature increased both $\omega_{e,i}$ and $\omega_{a,o}$ Eq. (19). As a result of the offsetting effects, the dehumidifier effectiveness finally affected slightly with the inlet desiccant temperature increasing. As shown in Fig. 7a and b, increasing the length of the structural packing from L=0.5 m to L=1.0 m enhanced the humidity reduction and dehumidifier effectiveness about 1.36 times.

5.2.4. Effect of inlet air flow rate on the performance

The effect of air flow rate on the humidity reduction and humidity effectiveness is shown in Fig. 8a with L=1.0 m and Fig. 8b with L=0.5 m. As indicated by the figures, the humidity reduction and dehumidifier effectiveness decreased with increasing air flow rate. Eqs. (18) and (19) indicated that humidity reduction and effectiveness decreased with increasing the outlet air humidity ratio. When the air flow rate increased, the outlet air humidity ratio increased, due to the reduced

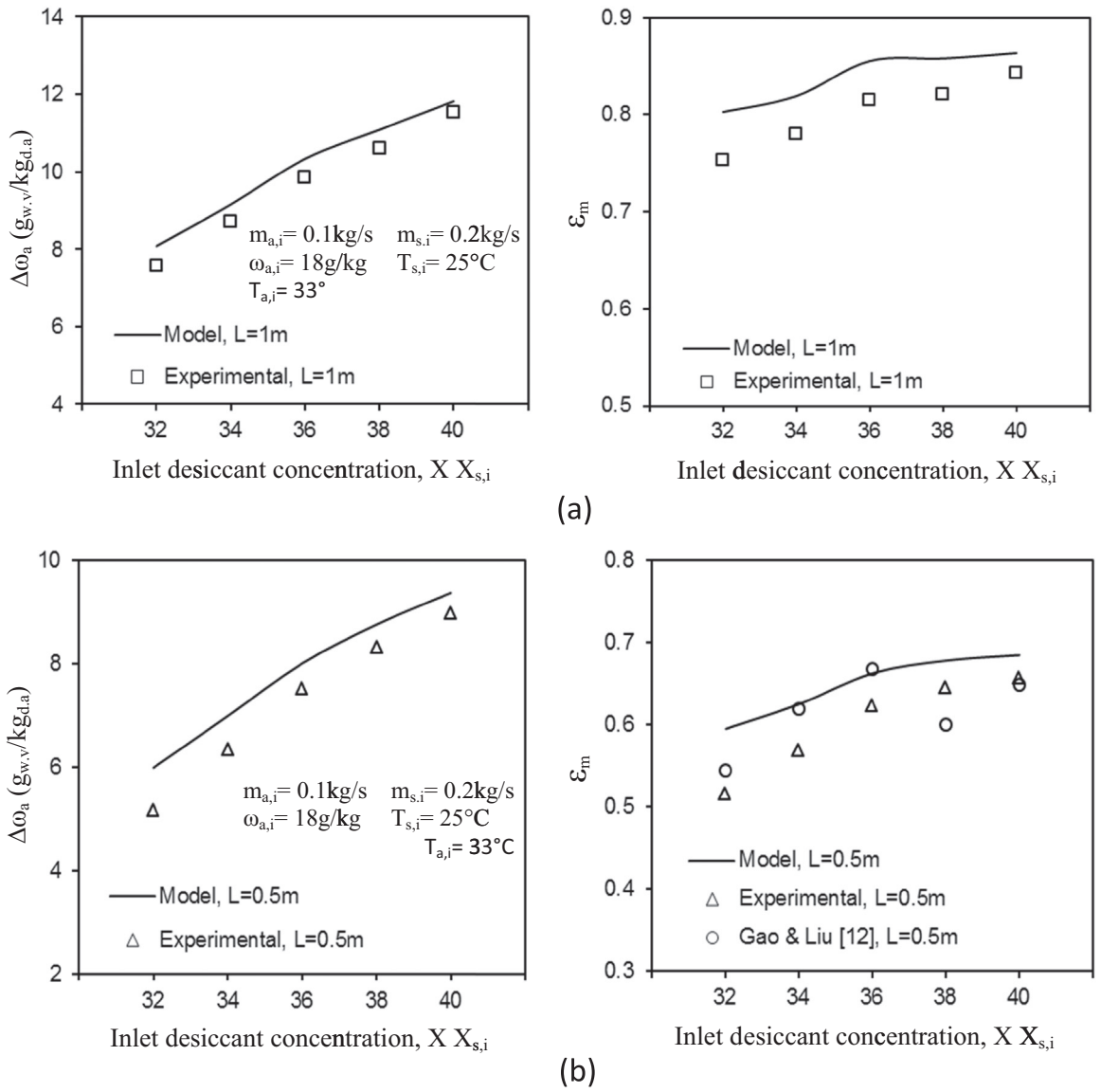

Fig. 6. Influence of inlet desiccant concentration on humidity reduction and dehumidifier effectiveness: (a) L=1.0 m and (b) L=0.5 m.

residence time for the air in the dehumidifier. This is in good agreement with Gao and Liu [12], as shown in Fig. 8b. The figures show also that increasing the length of structural gauze packing slides from L=0.5 m to L=1.0 m increased the humidity reduction and dehumidifier effectiveness about 44%.

5.2.5. Effect of inlet air humidity ratio on the performance

Fig. 9a and b shows the effect of the inlet air humidity ratio on the dehumidifier mass transfer performance. It is clear that the humidity reduction increases with the inlet air humidity ratio increasing, whereas the dehumidifier effectiveness slightly increases with it, especially at the high humidity ratio. The effect on the humidity reduction was caused by the increased average water vapor pressure difference between the air and the desiccant with increasing inlet air humidity ratio. The effect on the dehumidifier effectiveness lay in increasing the inlet air humidity ratio. As shown in Fig. 9a and b, increasing the length of the packing slides from L=0.5 m to L=1.0 m enhanced the humidity reduction and dehumidifier effectiveness about 1.29 times.

5.2.6. Effect of inlet air temperature on the performance

The effect of inlet air temperature on the dehumidifier performance is shown in Fig. 10a and b. The humidity reduction and dehumidifier effectiveness were almost weak affected by the inlet air temperature. The heat capacity of the liquid desiccant is much higher than the heat capacity of the air. So, increasing the inlet air temperature affected slightly the liquid

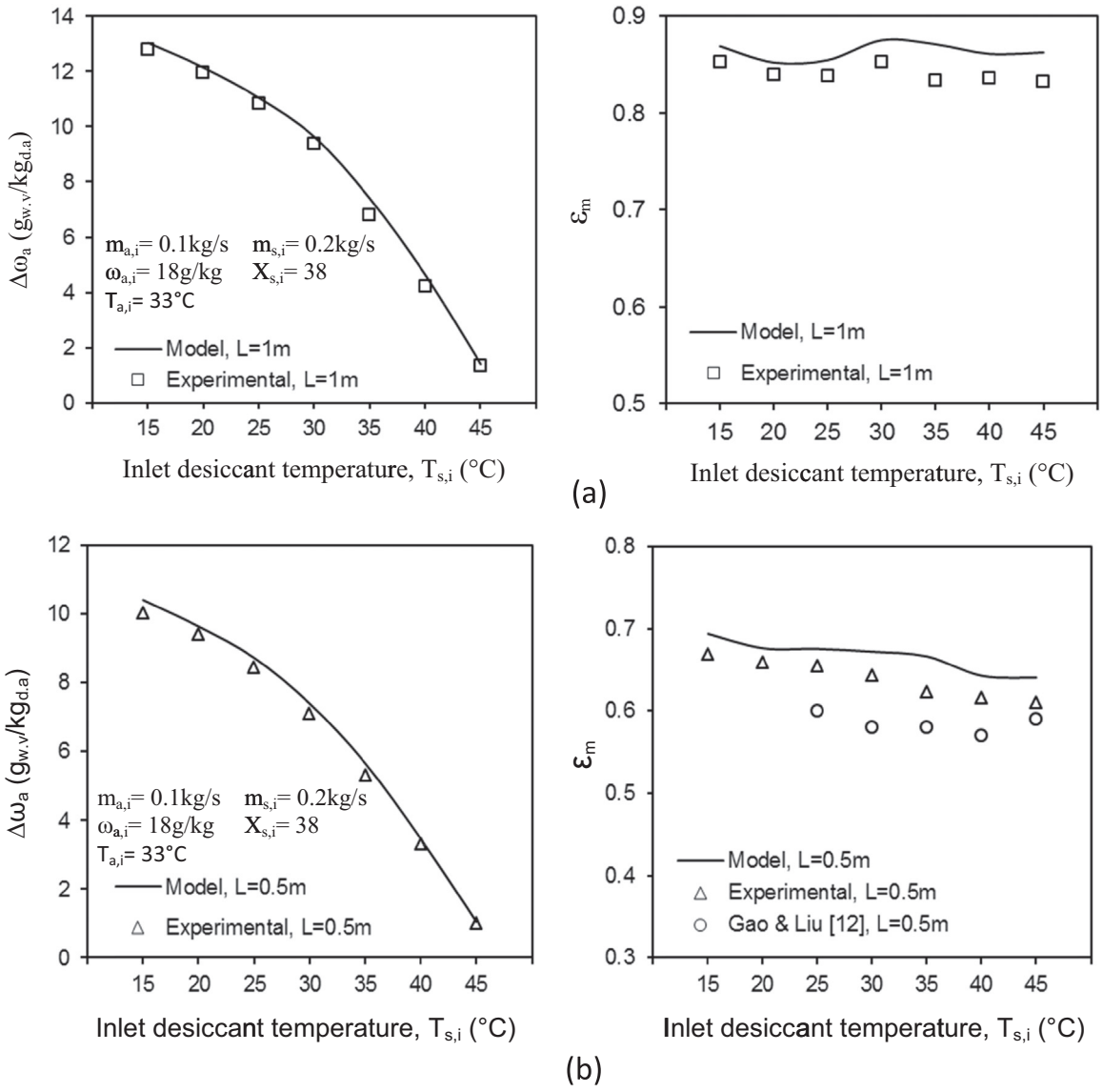

Fig. 7. Influence of inlet desiccant temperature on humidity reduction and dehumidifier effectiveness: (a) L=1.0 m and (b) L=0.5 m.

desiccant temperature. In turn, the average water vapor pressure difference between air and desiccant can be neglected in the dehumidifier. On the other hand, increasing the length of the gauze packing slides from L=0.5 m to L=1.0 m enhanced the humidity reduction and dehumidifier effectiveness about 34%, as shown in the figures.

Many previous studies investigating the packed bed dehumidifier defined NTU as:

$$NTU = \frac{\alpha_m A}{\dot{m}_\alpha}$$

As indicated by the equation NTU is the function of mass transfer coefficient α_m, total mass transfer area A and air flow rate $\dot{m}_a$.

The overall mass transfer area A, when the packing is fully wet, can be expressed as:

$$A = a.V$$

where, a is the specific area of packing per volume, and V is the volume of the packing material in the dehumidifier.

In present paper NTU is constant at value of 4.2 in Figs. 5, 6, 7, 9 and 10 with a constant air flow rate at 0.1 kg/s while, in Fig. 8, NTU ranges from 3.3 to 4.9.

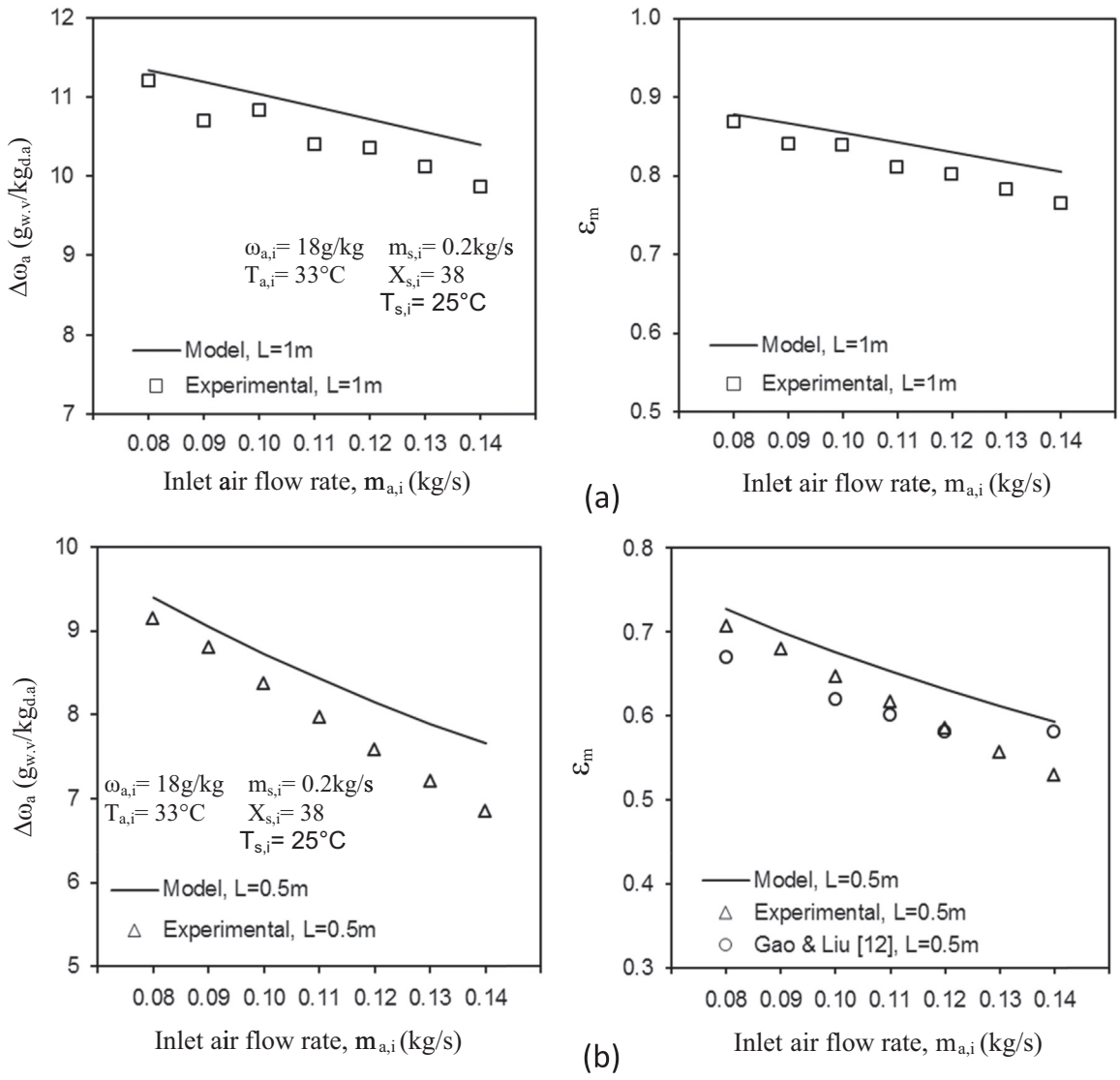

Fig. 8. Influence of inlet air flow rate on humidity reduction and dehumidifier effectiveness: (a) L=1.0 m and (b) L=0.5 m.

5.3. *Energy and mass balance for verification the experimental results*

The driving force for the mass transfer is the difference between the air vapor pressure and the equilibrium vapor pressure. The equilibrium vapor pressure increases with higher temperature. Hence, the mass transfer rate depends on temperature. Because of the involved heat of sorption, the heat transfer depends on the latent load of the mass transfer. Heat and mass transfer are therefore coupled. For a perfect experimental set up, the water vapor loss from the moist air is absorbed by the liquid desiccant in the dehumidifier. At the present experimental work, the liquid desiccant absorb water vapor about 4.5% more than what lost from the moist air at the following inlet conditions; air flow rate 0.1 kg/s, air temperature 33 °C, air humidity ratio 18 g/kg, desiccant flow rate 0.2 kg/s, desiccant temperature 25 °C and desiccant concentration 38%. This is due to some leakage of water vapor from the ambient air. Accordingly, the experimental energy loss between the desiccant and air is 8.2%.

5.4. *Comparison of current results with those reported in the literature*

The effects of the six inlet parameters on the humidity reduction and the dehumidifier effectiveness of the present study and experimental results reported in the literature are summarized in Table 3. The following observations can be made from Table 3:

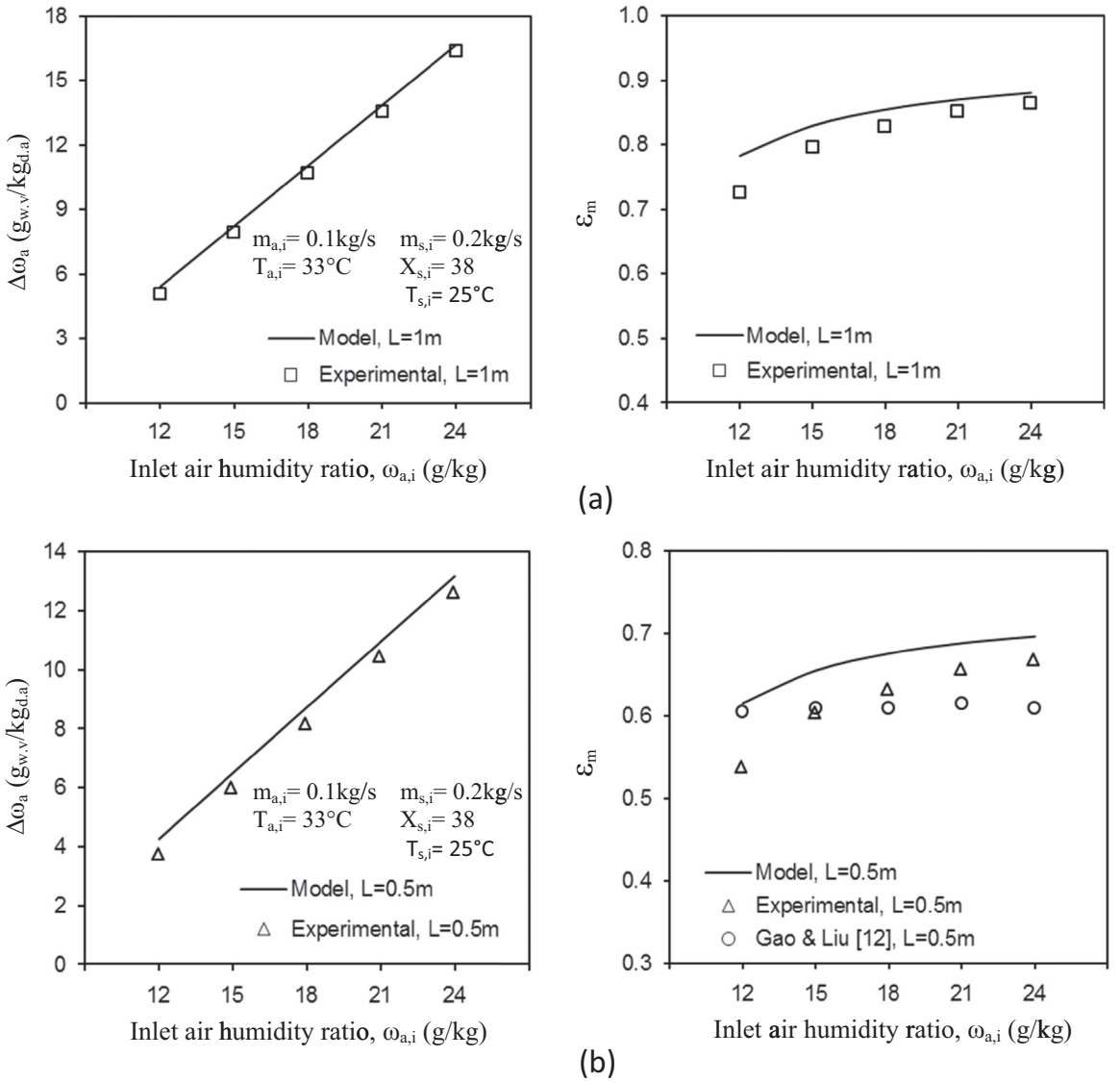

Fig. 9. Influence of inlet air humidity ratio on humidity reduction and dehumidifier effectiveness: (a) L=1.0 m and (b) L=0.5 m.

1. Lower $m_{s,i}/m_{a,i}$ ratios are preferred to reduce carryover. Some designs such as packed towers with random packing, inherently require high $m_{s,i}/m_{a,i}$ ratios.
2. There is a good agreement between the dehumidification effectiveness of the present study and those of studies using LiCl. The dehumidification effectiveness for these studies [12,26,30] lies in the range 0.3–0.9, and the present study lies in the range 0.69–0.87.
3. Maximum humidity reduction of air has been reported to be 18 g/kg, depending on initial humidity ratio of the air, the dehumidifier characteristics and the inlet vapor pressure of the desiccant, while in the present study the humidity reduction is 16.4 g/kg.
4. The pressure drop (Pa/m) in the dehumidifier has been reported to be as the following, Elsarrag et al. [31] (35–140), Longo and Gasparella [30] (25–45), Oberg and Goswami [32] (30–210), Liu and Jiang [33] (115–300) and Gao and Liu [12] (105–195) while in this study (8–35). The slides arrangement of packing used in this study produced low pressure drop ranging compared to the experimental pressure drop of selected dehumidifiers from the literature.

6. Conclusion

This paper theoretically and experimentally studies the mass transfer process between the air and the desiccant when they cross flow through channel gauze structured packing dehumidifier. Humidity reduction and dehumidifier effectiveness

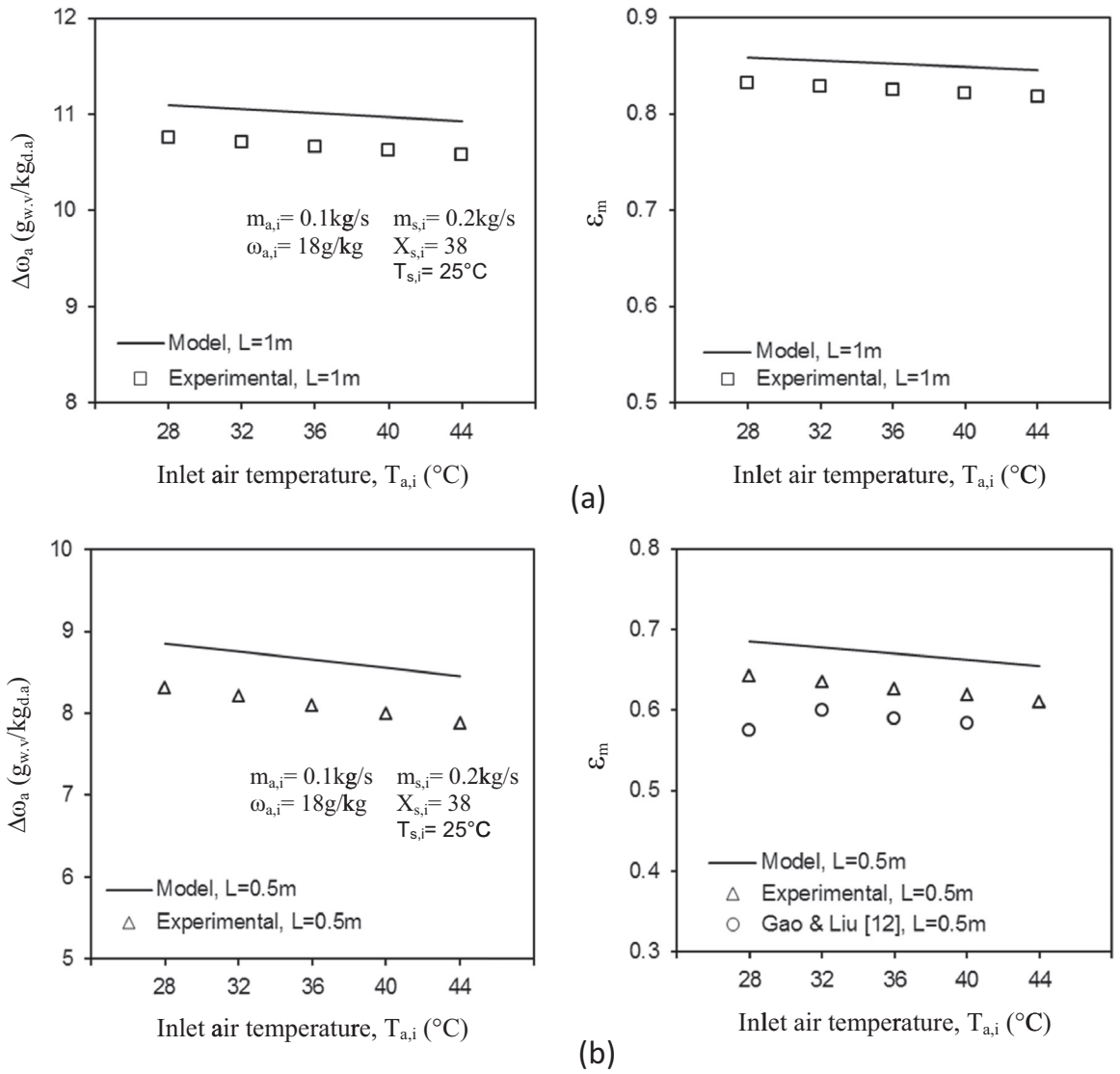

Fig. 10. Influence of inlet air temperature on humidity reduction and dehumidifier effectiveness: (a) L=1.0 m and (b) L=0.5 m.

were used as the performance indices of the mass transfer process. Generally, inlet parameters have the same trends in affecting the performance of the present dehumidifier and the experimental results reported in the literature. The main conclusions that can be derived from this study can be summarized as follows:

1. In experimental investigation, it was found that the performance parameters did not show any dependency on the liquid flow rate when liquid to air flow rate ratios ($m_{s,i}/m_{a,i}$) is equal or greater than 2.0. The effect of the specific area of packing per volume on the humidity reduction is extremely high while its effect on the pressure drop is affected slightly.
2. Increasing the length of packing from 0.5 m to 1.0 m enhanced the humidity reduction and dehumidifier effectiveness about 1.33 times.
3. Using structured packing arranged as straight sheets produced significantly low pressure drop compared to the experimental pressure drop of selected dehumidifiers from the literature, in turn, more energy saving in air stream.

Table 3
Experimental performance of liquid desiccant dehumidifiers.

Source of data	Desiccant			Air			$m_{s,i}/m_{a,i}$	ε_m	Pressure drop, ΔP (Pa/m)	Remarks
	Type	$T_{s,I}$ (°C)	$X_{s,i}$ (%)	$T_{a,i}$ (°C)	$\omega_{a,I}$ (g/kg)	$\Delta\omega_a$ (g/kg)				
Pietruschka et al. [34]	LiCl	27	43	26	11.6	4.2	0.46			SP, cross flow
Elsarrag et al. [31]	TEG	29–35	92		17–26	5.5 to11	1.9–2.3	0.45–0.85	35–140	SP, CF
Fumo and Goswami [26]	LiCl	30.1	34.6	30.1	18.0	7.6	6.88	0.75–0.84		RP, CF, 210 m^2/m^3
		30	34.3	30.2	18.1	7.3	4.04			
		30.5	34.4	40.1	18.0	6.5	5.31			
		30.1	33.9	30.3	14.2	3.9	5.17			
Longo and Gasparella [30]	LiCl	23.4–24	39.2–40.6	24.3–37.6	7.3–23.3	2–17	0.23–2.6	0.3–0.9	25–45	RP, CF
	LiBr	23.7	51.9–53.9	23.6–36.7	8.2–22.8	3–18	0.35–3.0	0.3–0.9		
	KCOOH	21.9–24.8	72.8–74	22.6–35.8	8.8–20.7	2–13.5	0.2–2.5	0.3–0.9		
Oberg and Goswami [32]	TEG	24–36	94–96	24–36	11–23	8.5 to10	4.5–11.0	0.8–0.9	30–210	RP, CF
Abdul-Wahab et al. [35]	TEG	28–45	93–98	25.4–44		0.1 to 0.24	0.06–2.07	0.1–0.7		SP of wood, CF,77–200 m^2/m^3
		31	95.6	31		0.15 to 0.2	0.11	0.16–0.4		
Liu and Jiang [33]	LiBr	20.1–29.5	42.6–54.8	24.7–33.9	10–21		1.0–2.13	0.38–0.68	115–300	SP, cross flow, 396 m^2/m^3
Gao and Liu [12]	LiCl	22–50	32–40	27–38	9.3–21.3		1.25–3.25	0.41–0.75	105–195	SP, cross flow, 396 m^2/m^3
Present study	**LiCl**	**25–45**	**32–40**	**28–44**	**9–24**	**1.4–16.4**	**0.63–3.75**	**0.69–0.87**	**8–35**	**SP, cross flow, 400 m^2/m^3**

RP, random packing; SP, structured packing; CF, counter flow.

References

[1] P. Biswas, S. Kim, A.F. Mills, A compact low pressure drop desiccant bed for solar air conditioning applications: analysis and design, J. Sol. Energy Eng. 106 (1984) 153–158.
[2] S. Jain, P.L. Dhar, S.C. Kaushik, Evaluation of liquid desiccant based evaporative cooling cycles for typical hot and humid climates, Heat Recover. Syst. CHP 14 (1994) 621–632.
[3] P.L. Dhar, S.C. Kaushik, S. Jain, Thermodynamic analysis of desiccant-augmented evaporative cooling cycles for Indian conditions, ASHRAE Trans. 101 (1995) 735–749.
[4] P. Gandhidasan, A simplified model for air dehumidification with liquid desiccant, Sol. Energy 76 (2004) 409–416.
[5] M.M. Bassuoni, An experimental study of structured packing dehumidifier/regenerator operating with liquid desiccant, Energy 36 (2011) 2628–2638.
[6] A.A. Kinsara, M.M. Elsayed, O.M. Al-Rabghi, Proposed energy-efficient air-conditioning system using liquid desiccant, Appl. Therm. Eng. 16 (1996) 791–806.
[7] W. Kessling, E. Laevemann, M. Peltzer, Energy storage in open cycle liquid desiccant cooling systems, Int. J. Refrig. 21 (1998) 150–156.
[8] D.G. Waugaman, A. Kini, C.F. Kettleborough, A review of desiccant cooling systems, J. Energy Resour. Technol. 115 (1993) 1–8.
[9] S. Jain, P.K. Bansal, Performance analysis of liquid desiccant dehumidification systems, Int. J. Refrig. 30 (2007) 861–872.
[10] L. Zhang, E. Hihara, F. Matsuoka, C. Dang, Experimental analysis of mass transfer in adiabatic structured packing dehumidifier/regenerator with liquid desiccant, Int. J. Heat Mass Transf. 53 (2010) 2856–2863.
[11] P. Gandhidasan, Prediction of pressure drop in a packed bed dehumidifier operating with liquid desiccant, Appl. Therm. Eng. 22 (2002) 1117–1127.
[12] W.Z. Gao, J.H. Liu, P. ChengY, X.L. Zhang, Experimental investigation on the heat and mass transfer between air and liquid desiccant in a cross-flow dehumidifier, Renew. Energy 37 (2012) 117–123.
[13] M.R.H. Abdel-Salam, G. Ge, M. Fauchoux, R.W. Besant, C.J. Simonson, State-of-the-art in liquid-to-air membrane energy exchangers (LAMEEs): a comprehensive review, Renew. Sustain. Energy Rev. 39 (2014) 700–728.
[14] M.R.H. Abdel-Salam, M. Fauchoux, G. Ge, R.W. Besant, C.J. Simonson, Expected energy and economic benefits, and environmental impacts for liquid-to-air membrane energy exchangers (LAMEEs) in HVAC systems: a review, Appl. Energy 127 (2014) 202–218.
[15] G. Ge, M.R.H. Abdel-Salam, R.W. Besant, C.J. Simonson, Research and applications of liquid-to-air membrane energy exchangers in building HVAC systems at university of Saskatchewan: a review, Renew. Sustain. Energy Rev. 26 (2013) 464–479.
[16] M.R.H. Abdel-Salam, R.W. Besant, C.J. Simonson, Sensitivity of the performance of a flat-plate liquid-to-air membrane energy exchanger (LAMEE) to the air and solution channel widths and flow maldistribution, Int. J. Heat Mass Transf. 84 (2015) 1082–1100.
[17] A.H. Abdel Salam, C. Simonson, State-of-the-art in liquid desiccant air conditioning equipment and systems, Renew. Sustain. Energy Rev. 58 (2016) 1152–1183.
[18] S. Bergero, A. Chiari, On the performances of a hybrid air-conditioning system in different climatic conditions, Energy 36 (2011) 5261–5273.
[19] M.R.H. Abdel-Salam, R.W. Besant, C.J. Simonson, Design and testing of a novel 3 fluid liquid to air membrane energy exchanger (3 fluid LAMEE), Int. J. Heat Mass Transf. 92 (2016) 312–329.
[20] M.R.H. Abdel-Salam, R.W. Besant, C.J. Simonson, Performance testing of a novel 3 fluid liquid to air membrane energy exchanger (3 fluid LAMEE) under desiccant solution regeneration operating conditions, Int. J. Heat Mass Transf. 95 (2016) 773–786.
[21] M.R.H. Abdel Salam, G. Ge, R. Besant, C. Simonson, Experimental study of effects of phase change energy and operating parameters on performances of two fluid and three fluid liquid to air membrane energy exchangers, ASHRAE Trans. 122 (2016). Part 1.
[22] C.Q. Ren, M. Tu, H.H. Wang, An analytical model for heat and mass transfer processes in internally cooled or heated liquid desiccant-air contact units, Int. J. Heat Mass Transf. 50 (2007) 3545–3555.
[23] Y. Yin, X. Zhang, G. Wang, L. Luo, Experimental study on a new internally cooled/heated dehumidifier/regenerator of liquid desiccant systems, Int. J. Refrig. 31 (2008) 857–866.
[24] M.R. Conde, Properties of aqueous solutions of lithium and calcium chlorides: formulations for use in air conditioning equipment design, Int. J. Therm. Sci. 43 (2004) 367–382.
[25] A.A.M. Hassan, M.S. Hassan, Dehumidification of air with a newly suggested liquid desiccant, Renew. Energy 33 (2008) 1989–1997.
[26] N. Fumo, D.Y. Goswami, Study of an aqueous lithium chloride desiccant system: air dehumidification and desiccant regeneration, Sol. Energy 72 (2002) 351–361.
[27] Y. Yang, Experimental Study on the Characteristic of Liquid Desiccant Dehumidification System (Master Thesis), Department of Thermal Engineering, Tian Jin University, China, 1999.
[28] S. Patnaik, T.G. Lenz, G.O.G. Lof, Performance studies for an experimental solar open-cycle liquid desiccant air dehumidification system, Sol. Energy 44 (1990) 123–135.
[29] Y.H. Zurigat, M.K. Abu-Arabi, S.A. Abdul-Wahab, Air dehumidification by triethylene glycol desiccant in a packed column, Energy Convers. Manag. 45 (2004) 141–155.
[30] G.A. Longo, A. Gasparella, Experimental and theoretical analysis of heat and mass transfer in a packed column dehumidifier/regenerator with liquid desiccant, Int. J. Heat Mass Transf. 48 (2005) 5240–5254.
[31] E. Elsarrag, E.M. Elmagzoub, S. Jain, Design guidelines and performance study on a structured packed liquid desiccant air conditioning system, HVACR J. 11 (2005) 319–337.
[32] V. Oberg, D.Y. Goswami, Experimental study of the heat and mass transfer in a packed bed liquid desiccant air dehumidifier, ASME J. Sol. Energy Eng. 120 (1998) 289–297.
[33] X. Liu, Y. Jiang, K. Qu, Analytical solution of combined heat and mass transfer performance in a cross-flow packed bed liquid desiccant air dehumidifier, Int. J. Heat Mass Transf. 51 (2008) 4563–4572.
[34] D. Pietruschka, U. Eicker, M. Huber, J. Schumacher, Experimental performance analysis and modeling of liquid desiccant cooling systems for air conditioning in residential buildings, Int. J. Refrig. 29 (2006) 110–124.
[35] S.A. Abdul-Wahab, Y.H. Zurigat, M.K. Abu-Arabi, Predictions of moisture removal rate and dehumidification effectiveness for structured liquid desiccant air dehumidifier, Energy 29 (2004) 19–34.